ACS Catalysis

Research Article

pubs.acs.org/acscatalysis

Dinuclear Iridium(III) Complexes Containing Bibenzimidazole and Their Application to Water Photoreduction

Jian-Guang Cai,[†,‡] Zhen-Tao Yu,*[,†] Yong-Jun Yuan,[†] Feng Li,[‡] and Zhi-Gang Zou[†]

[†]National Laboratory for Infrared Physics, Chinese Academy of Sciences; Eco-Materials and Renewable Energy Research Center, Department of Materials Science and Engineering, Nanjing University, Kunshan Innovation Institute of Nanjing University, No. 22, Hankou Road, Nanjing, Jiangsu 210093, P. R. China

[‡]School of Chemical Engineering, Nanjing University of Science and Technology, No. 200, Xiaolingwei Street, Nanjing, Jiangsu 210094, P. R. China

Supporting Information

ABSTRACT: An efficient three-component catalytic system for visible-light-induced production of hydrogen from water was developed based on new dinuclear iridium photosensitizers (PSs), $[Ir(tfdpyb)Cl]_2(BiBzIm)$ (**P1**) and $[Ir(tfmppy)_2]_2BiBzIm$ (**P2**) [tfdpyb = 1,3-di(2-pyridyl)-4,6-bis(trifluoromethyl)benzene, tfmppy = 2-(4-(trifluoromethyl)phenyl)-pyridine, BiBzIm = 2,2′-bibenzimidazole]. These iridium complexes were fully characterized by ^1H NMR and ESI-MS, and their photophysical properties and electrochemical behaviors were also investigated. To compare with this new type of iridium compounds, the mononuclear analogues Ir(tfdpyb)(BiBzImH)Cl (**P3**), $Ir(tfmppy)_2(BiBzImH)$ (**P4**), and Ir(dpyx)(BiBzImH)Cl (**P5**) (dpyx = 1,3-di(2-pyridyl)-4,6-dimethylbenzene) were also synthesized. The absorption spectra of dinuclear and mononuclear complexes are similar mainly in terms of their shape in the visible-light region, but as expected, the dinuclear species are more intense (approximately twice) compared with the corresponding mononuclear compounds. These complexes were tested as PSs with regard to their capacity to reduce water in the photocatalytic system for hydrogen production together with a series of water reduction catalysts and triethanolamine (TEOA) as a sacrificial electron donor. Turnover numbers up to 3780 for the dinuclear iridium complex **P1** and 1020 for the mononuclear iridium compound **P3** were obtained under the identical conditions. The results indicate that dinuclear iridium compounds can behave as PSs to be used for reducing water to hydrogen, and their activity was superior to that of the mononuclear compounds in this system. This work provides us a more general architectural guideline for constructing metal complexes as light-harvesting materials for visible-light-induced hydrogen production.

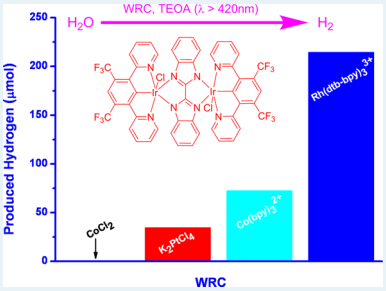

KEYWORDS: *hydrogen evolution, iridium, photochemistry, photosensitizer, water splitting*

INTRODUCTION

Transition-metal-based photoactive complexes are garnering increasing amounts of interest as important components, i.e., efficient light-harvesting photosensitizers (PSs), in artificial systems for solar energy conversion.[1−6] A key characteristic that makes these complexes unique is their capacity to absorb low-energy visible light and thereby access the energetic metal-to-ligand charge-transfer excited states capable of photoactivation.[7−9] In designing such synthetic light-harvesting species for solar energy conversion strategies, it is imperative to explore systems that maximize the efficiency of photon absorption, whereas the construction of structural complexity is to be minimized.[10−14] Among these systems, iridium-containing complexes carrying bidentate ligands, such as 2,2′-bipydirdine and their derivatives, express this unusual utility due to their relevant photophysical and photoredox properties for such applications.[15−23] The development of such chromophores suffers from relatively weak absorption in the visible region, which impairs the overall functional performance and efficiency of the solar energy conversion system. The tailoring of materials under synthetic design control will provide unique opportunities to alleviate the above-mentioned limitations. It has been widely recognized that the electronic properties and chemical attributes of the iridium complexes can be finely tuned by systematic control of the nature and position of the appropriate functional substituents on the chelating ligands that are bound to the metal center.[24] The ligand properties can be manipulated to design metal complexes with particular functionality and may also strongly influence the course and efficiency of the photochemical electron transfer involving the metal complexes.

Through the use of transition metal catalysts and an external electron donor, the photosensitizing behavior of many iridium complexes has typically been evaluated for the photogeneration of hydrogen using mononuclear bis-cyclometalated complexes, $[Ir(C^N)_2(N^N)]^+$ (C^N = 2-arylpyridine; N^N = neutral bipyridyl ligands), because of their relatively facile synthetic accessibility and their good efficacy. Unfortunately, a general

Received: March 5, 2014
Revised: April 24, 2014
Published: May 2, 2014

problem with the use of this type of light-absorbing molecule is the inherently low stability caused by the easy rupture of weak Ir−N bonding in the Ir-bipyridyl moiety, which leads to the termination of catalysis during irradiation.[25] Improving the stability properties can be achieved to a certain degree by structural modifications, such as the introduction of vinyl group or pyridyl pendants at the bipyridyl ligand backbone of the iridium complex.[26−28] Additionally, an alternative approach has been developed to minimize the photolability of the chromophore using neutral tris-cyclometalated iridium complexes.[29,30] The implementation of tris-cyclometalation provides such complexes with improved long-term stability along with extensive electronic couplings between the d-orbital of the Ir center and π-orbital of the ligands. In this approach, the Ir−C bond between the central Ir metal and the ligand is sufficiently strong to survive the necessary changes in oxidation state that occur during a photochemical reaction. Clearly, the exploration of complexes with new structural motifs aimed to facilitate photoinduced electron-transfer processes is worth pursuing to contribute to a better understanding of the structure−activity correlations of this class of materials.

In the course of our studies related to the design and development of new potential light-harvesting materials that can play an active role in hydrogen production, we have become interested in conjugated organic unit-bridged dimetallic iridium assemblies with the intention of achieving improved optical characteristics and the associated performance improvements in such processes. Dinuclear complexes are of particular interest because they display exquisite electronic and photochemical properties that are distinctly different from those of their mononuclear counterparts.[31−42] However, the use of this class of compounds for fundamental studies of the photochemical conversion of solar energy remains limited, most likely due to the synthetic difficulties involved. In the design of such systems, the suitable bridging ligands are responsible for separating the photoactive terminals and ensuring electronic coupling between the metal partners.

The use of 2,2′-bibenzimidazole ($BiBzImH_2$) has been extensively studied as a symmetrical two-bidentate ligand for the formation of dinuclear complexes with five-membered chelate rings, particularly with Ru, either as heterometallic or homometallic systems.[43−46] Related complexes of the $BiBzImH_2$ ligand exhibit enhanced electron transport ability and notable electronic coupling between two metals due to the great electron motilities of the bridging ligand. These studies motivated us to explore $BiBzImH_2$ as a bridging ligand in connection with pairs of iridium complex fragments for the construction of appealing dinuclear iridium complexes, which is appropriate from structural and photophysical viewpoints. In this context, two new dinuclear iridium complexes (compounds **P1** and **P2** shown in Scheme 1), which use a $BiBzImH_2$ ligand to link together two cyclometalated Ir(III) species, have been synthesized. The electrochemical and photophysical properties measured for the dinuclear compounds are discussed in comparison with those obtained for the mononuclear analogues **P3**, **P4**, and **P5**, containing one terdentate cyclometalating ligand that can bind to iridium in an N^C^N coordination mode or two ortho-metalating ligands. The resulting dinuclear compounds exhibit significantly different photophysical and electrochemical attributes with respect to their corresponding mononuclear complexes. In particular, the present report indicates that photocatalytic hydrogen production is possible using such dinuclear complexes as **P1** and **P2** as the active PS components and is rationalized in terms of the photophysical properties of the dinuclear complexes.

Scheme 1. Chemical Structure of Iridium Compounds P1−P5

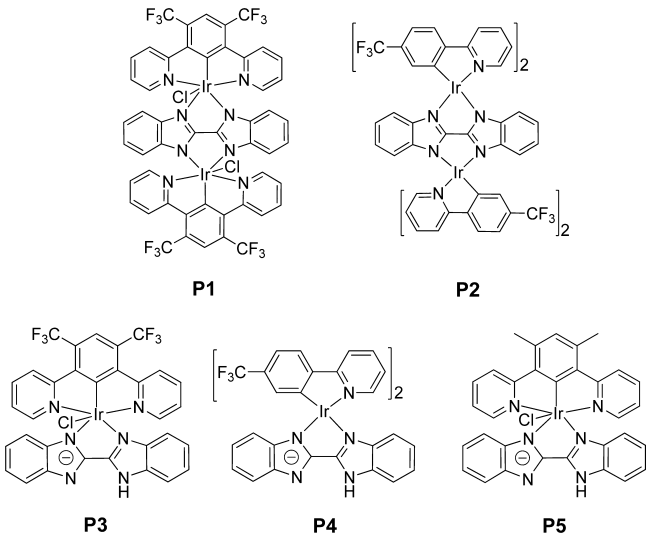

RESULTS AND DISCUSSION

Synthesis and Characterization. To date, few examples of dinuclear iridium complexes incorporating a π-conjugated bridging ligand have been reported in the literature, and all of these complexes are cationic.[31−42] The straightforward synthetic strategy used in the present study to prepare the target complexes and reference complexes is outlined in Scheme 2. A similar two-step strategy has previously been successfully applied to the synthesis of mononuclear iridium complexes. The molecules 1,3-di(2-pyridyl)-4,6-bis(trifluoromethyl)benzene (tfdpybH), 1,3-di(2-pyridyl)-4,6-dimethylbenzene (dpyxH), and 2-(4-(trifluoromethyl)phenyl)-pyridine (tfmppy) were prepared as the cyclometalating ligands according to a literature procedure by the traditional palladium-catalyzed Still cross-coupling method.[47,48] As reported, the complexation of 1,3-di(2-pyridyl)benzene with iridium primarily preferred a bidentate mode of coordination (C^N), rather than the terdentate structure (N^C^N). The introduction of substituents at the C4 and C6 positions of the central ring resulted in the formation of the terdentate-bound product.[49] The use of dpyxH allows us to prepare different iridium complexes for understanding the effects of substituents on the photophysical properties of the desired complexes.

The first step involves the preparation of a chloride-bridged Ir(III) dimer as the precursor by reacting the cyclometalating ligand with $IrCl_3{\cdot}3H_2O$ in aqueous 2-ethoxyethanol according to the Nonoyama protocol. We attempted the synthesis of the target chloro complexes of iridium(III) from the conventional bridge-splitting reaction of the respective dichloro-bridged intermediates with ca. 2.2 equiv of $BiBzImH_2$ in the presence of a proton scavenger, Na_2CO_3, in CH_2Cl_2/CH_3OH (v/v = 1:1) under reflux. The reaction of $BiBzImH_2$ with the dimer intermediate of either tfdpybH or tfmppy led to mixtures of mono- and dinuclear iridium complexes, which were easy to separate by a silica column to obtain the resulting iridium complexes $[Ir(tfdpyb)Cl]_2(BiBzIm)$ (**P1**), $[Ir(tfmppy)_2]_2BiBzIm$ (**P2**), Ir(tfdpyb)(BiBzImH)Cl (**P3**), and $Ir(tfmppy)_2(BiBzImH)$ (**P4**). In both reactions, the cyclo-

dx.doi.org/10.1021/cs500296s | ACS Catal. 2014, 4, 1953−1963

Scheme 2. Synthetic Route of Iridium Complexes P1−P5

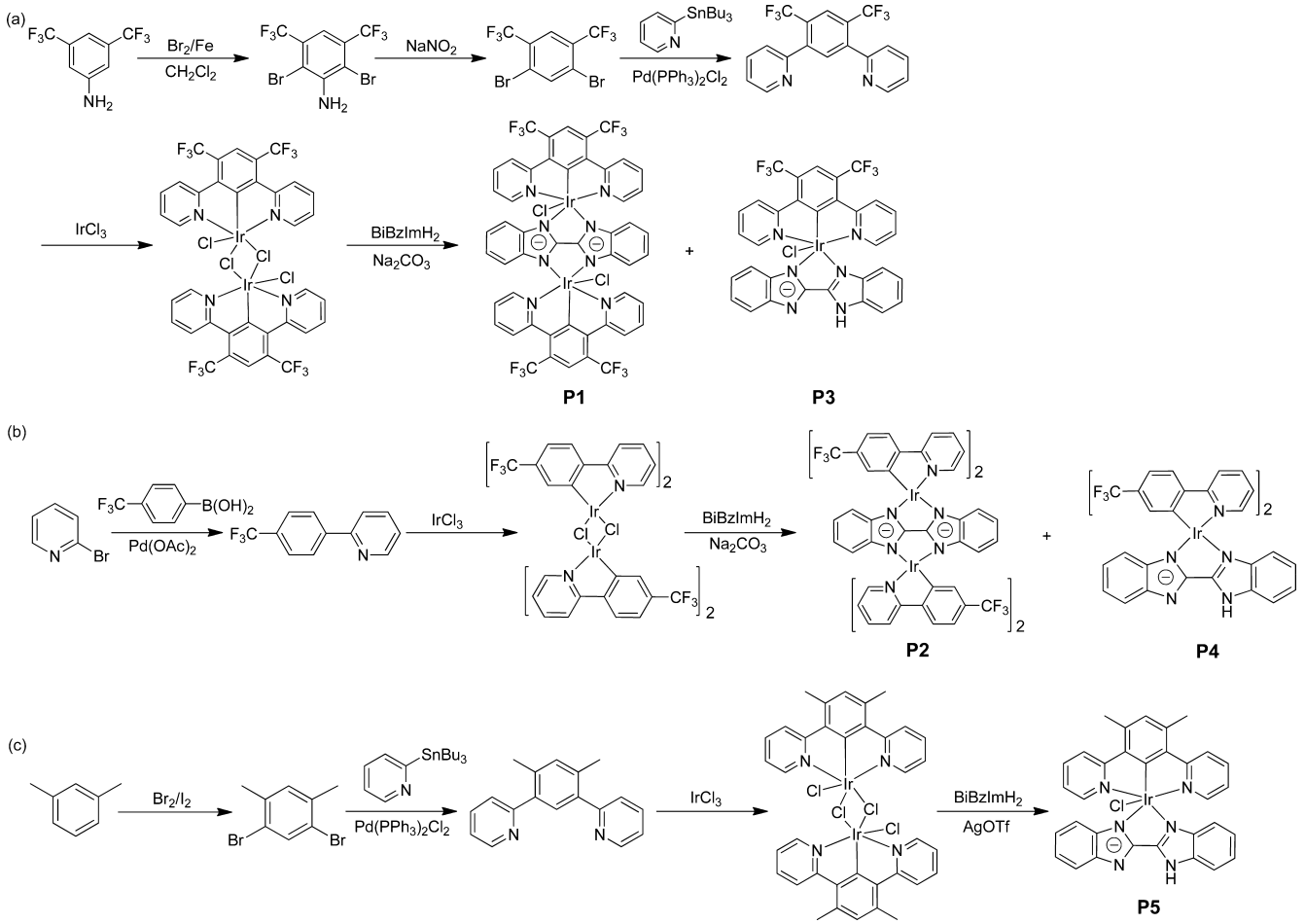

metalation proceeded smoothly and cleanly; however, attempts to prepare the related complexes containing the dpyxH ligand by the same method were unsuccessful. This finding was most likely due to the low solubility of the intermediate of dpyxH in the reaction solvent. In this case, even with a longer reaction time, mainly starting materials were recovered. In an alternative approach, the chlorides in the dimer precursor based on dpyxH were substituted with $BiBzImH_2$ in the presence of silver triflate (AgOTf) as a chloride scavenger,[50] followed by column chromatography, resulted in the clean formation of the mononuclear complex Ir(dpyx)(BiBzImH)Cl (**P5**) as a sole product. After the complexation, the protons on the $BiBzImH_2$ in all of the mononuclear complexes were partially deprotonated. Several attempts were made to react the mononuclear BiBzImH-containing complexes with the second metal center, such as $RhCl_3{\cdot}3H_2O$, $Pd(CH_3CN)_2Cl_2$, and K_2PtCl_4; however, efforts to form the heterometallic complexes by the second deprotonation with Na_2CO_3 were unsuccessful with the original mononuclear precursors being recovered. All of the iridium complexes were fully identified by a combination of ^1H NMR spectroscopy and mass spectrometry, the results of which are given in the Experimental Section, along with the single crystal X-ray diffraction of the chloride-free neutral complexes **P2** and **P4** containing tfmppy ligands (see the Supporting Information). Moreover, we used HRMS analyses to confirm that the negatively charged chloride group exists as an auxiliary ligand for the monodeprotonated iridium complexes **P3** and **P5** to complete the coordination sphere of the metals. After recrystallization, all samples were used for the following studies.

Photophysical Properties. The electronic absorption spectra of all of the complexes were recorded at room temperature in CH_2Cl_2 solutions, as shown in Figure 1. The absorption spectra of all of the complexes were featured by the most intense absorption bands in the ultraviolet region at wavelengths below 390 nm. This was attributed to the spin-allowed $^1\pi-\pi^*$ transition localized on both coordinated aromatic ligands within each complex, with reference to the

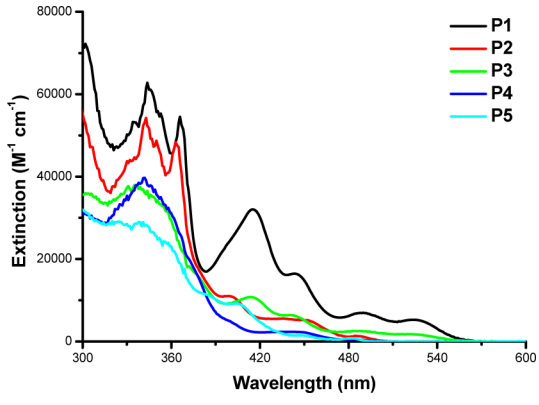

Figure 1. Electronic absorption spectra of all complexes (10^{-5} M) in CH_2Cl_2.

dx.doi.org/10.1021/cs500296s | ACS Catal. 2014, 4, 1953−1963

previous well-established photophysical studies of the iridium(III) diimine complexes.[31−42] These bands are less intense with maxima at lower energies (400−430 nm), most likely arising from the metal-to-ligand charge-transfer (MLCT) transition in the singlet manifold. It can be observed that the absorption spectra of dinuclear and mononuclear complexes are mainly similar in terms of their shape in the visible-light region; however, the dinuclear species are twice as intense compared to the corresponding mononuclear compound, which corresponds with the number of independent iridium-containing cores. Such an increase in absorption allows for the ability to capture more solar energy for this type of light-harvesting material. The lower-energy band tailed toward the lower energies from 460 to 550 nm. This band is likely associated with ^{3}MLCT; however, mixed with $^3\pi-\pi^*$ transition character, this is based on the observation of similar absorptions of the corresponding iridium complexes. The energy and intensity of the MLCT transitions is usually affected by the nature of ligand architectures in the iridium complexes. A difference in optical density and peak maxima for the present complexes is observed, indicating the electron-donation capability of the cyclometalating aryl moieties. The lower energy MLCT band in the terdentate N^C^N-containing complexes is significantly red-shifted with respect to the C^N-containing complexes. The red shift is due to a lowering of the energy of the acceptor ligand π^* orbital upon increased electronic delocalization (stability) throughout the entirety of the three aromatic rings of the N^C^N ligand.

The iridium(III) complexes display intense emission in solution at ambient air and room temperature, with the exception of **P5**. For mononuclear complex **P5**, no emission was detected, suggesting that it was sensitive to oxygen and subsequently completely quenched in air. The normalized luminescence spectra of these investigated complexes in an N_2-saturated methanol solution are presented in Figure 2, and the

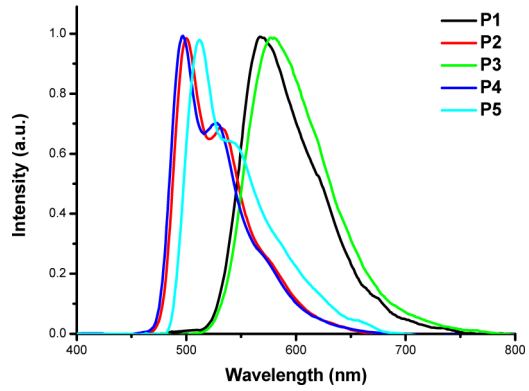

Figure 2. Emission spectra of all complexes (10^{-5} M, in N_2) in methanol at room temperature.

corresponding photophysical data are collected in Table 1. In contrast to the absorption spectra, the emission spectra of the dinuclear and mononuclear complexes differ significantly. The emission colors given by these iridium complexes range from green to orange (496−578 nm), with the emission energies in the order of **P4** > **P2** > **P5** > **P1** > **P3**. The color shifts depended on the organic ligand chromophores with the difference in the ligand field strength. The terdentate complexes **P1** and **P3** show a broad, structureless emission band centered at λ_{max} = 568 (**P1**) and 578 nm (**P3**), indicating that the emission can be attributed to the prevalent ^{3}MLCT state. The

Table 1. Photophysical and Electrochemical Properties of Studied Iridium Complexes P1−P5

PS	λ_{em}[a] (nm)	τ[b] [μs]	Φ[b] [%]	E_{ox}[c] [V]	E_{red}[c] [V]	E_{0-0}[d] [eV]
P1	568	0.29	11.8	+0.68	−0.89	2.23
P2	500, 532	1.28	37.7	+1.03	−1.45	2.42
P3	578	1.55	55.8	+0.73	−0.84	2.22
P4	496, 527	2.01	28.8	+0.81	−1.56	2.47
P5	512, 540 (sh)	0.22		+0.74	−1.07	2.51

[a]Measurements in air-equilibrated CH_3OH at room temperature. [b]Measurements in N_2 atmosphere in CH_3OH at room temperature. For **P5**, the fluorescence intensity was too low to quantify a quantum yield (Φ). [c]Redox potentials measured in deoxygenated CH_3CN with 0.1 M n-Bu_4NPF_6 as the supporting electrolyte; potentials measured vs Ag/AgCl coupled and converted to normal hydrogen electrode (NHE); only the first reduction and oxidation wave were shown. [d]E_{0-0} values were calculated from the intersection of the normalized absorption and the emission spectra.

change in maximum emission also indicated that the formation of the dinuclear complexes exert an influence on the energy of the emitting states. However, the photoluminescence spectra of complexes **P2** and **P4** have a similar shape and display vibronic-structured emission bands. The luminescence of terdentate complexes **P1** (λ_{max} = 568 nm) and **P3** (λ_{max} = 578 nm) are substantially red-shifted in comparison to those observed for complexes **P2** (λ_{max} = 500 nm) and **P4** (λ_{max} = 496 nm). As in the absorption spectra, this can be attributed to a lowering of the energy of the N^C^N ligand π^* orbital due to increased conjugation as a result of the introduction of an additional pyridyl ring compared to the bidentate cyclometalating ligand. Little shift in the value of λ_{max} was observed in the emission for these iridium complexes in CH_2Cl_2 under N_2 atmosphere. We also determined the excited-state lifetime (τ) and the absolute quantum yield (Φ) of the complexes in a dilute N_2-saturated CH_3OH solution (10^{-5} M), the results of which are summarized in Table 1. The values are consistent with those previously observed for cyclometalated iridium complexes.[31−42] The lifetimes of the dinuclear complexes **P1** (0.29 μs) and **P2** (1.28 μs) are notably shorter than those of their corresponding mononuclear complexes **P3** (1.55 μs) and **P4** (2.01 μs) under the same conditions.

Electron-transfer quenching of the excited states of complexes in solution at room temperature, with TEOA, $Co(bpy)_3^{2+}$, and $Rh(dtb\text{-}bpy)^{3+}$ acting as quenchers, were conducted to probe the influence of the excited state of the complexes on the quenching process. We detected the emission spectral changes upon the addition of increasing amounts of TEOA, $Co(bpy)_3^{2+}$, or $Rh(dtb\text{-}bpy)^{3+}$ to the acetone/water (4:1 v/v) solution of complexes **P1**−**P4** (see the Supporting Information). **P5** yielded notably weak emission in air-equilibrated solution and thus did not allow reliable quantification of the quenching process. The results of these experiments are presented in Table 2. Notably, all of the dinuclear and mononuclear iridium complexes **P1**−**P4** are easily oxidatively quenched by $Co(bpy)_3^{2+}$ or $Rh(dtb\text{-}bpy)^{3+}$, following good Stern−Volmer behavior. The terdentate complexes **P1** and **P3** can also be reductively quenched by TEOA following good Stern−Volmer behavior, whereas compounds **P2** and **P4** are not reductively quenched by TEOA, similar to other neutral cyclometalated iridium complexes.[29,30] The observed quenching behavior of **P1** or **P3** is similar to that observed for other charged complexes with

dx.doi.org/10.1021/cs500296s | ACS Catal. 2014, 4, 1953−1963

Table 2. Quenching Kinetics of Studied Iridium Complexes.[a]

PS	k_q $Co(bpy)_3^{2+}$ (M^{-1} s^{-1})	k_q $Rh(dtb\text{-}bpy)^{3+}$ (M^{-1} s^{-1})	k_q TEOA (M^{-1} s^{-1})
P1	1.59×10^{10}	2.00×10^{10}	2.62×10^{7}
P2	3.36×10^{9}	2.73×10^{9}	no quenching
P3	3.42×10^{10}	2.71×10^{9}	4.52×10^{9}
P4	6.96×10^{10}	1.94×10^{9}	no quenching
P5[b]			

[a]Measured in acetone/water (4:1 v/v) at room temperature. [b]**P5** gave very weak emission in the air-saturated solution.

an N^N ancillary ligand such as $[Ir(C^N)_2(N^N)]^+$.[21,22] The phenomenon is likely related to the fact that compounds **P1** and **P3** contain one monodentate halide ligand for possible interaction with TEOA in the quenching process. The results indicated that chromophores **P1** and **P3** undergo oxidative, as well as reductive, quenching of their respective excited states. The value of the quenching constant (k_q) for each complex with each of the two quenchers was determined from the lifetimes in the absence of quencher using the Stern–Volmer equation. The rate for quenching by $Co(bpy)_3^{2+}$ was at least 1 order of magnitude faster than the rate by TEOA for terdentate complexes, which is in agreement with the observation for the cases of charged complexes with an N^N ancillary ligand such as $[Ir(C^N)_2(N^N)]^+$.[18]

Electrochemical Properties. Electrochemical measurements were performed to determine the redox potentials of all five complexes in deoxygenated MeCN, the results of which are shown in Table 1. The electrochemical properties of these iridium compounds are too complex to understand exactly the oxidation and reduction involving the transfer of electrons, which have been observed in previous reports on the metal complexes based on the BiBzIm ligand.[43−46] In this study, only the first oxidation and reduction were discussed, which play an important role in the photochemical processes. The cyclic voltammograms of the five compounds exhibit irreversible first oxidation potentials in the range of 0.68−1.03 V versus NHE. According to the previously published works concerning analogous iridium cyclometalates and on the basis of the quantum mechanical calculations (vide infra), the oxidation could mainly be associated with iridium-centered orbitals and σ band Ir−C orbitals derived from the removal of an electron belonging to the highest occupied molecular orbital (HOMO). The first oxidation potential of the dinuclear compound **P1** ($E_{1/2}$ = 0.68 V vs NHE) is lower than that of the mononuclear compound **P3** ($E_{1/2}$ = 0.73 V vs NHE), which may be due to the electronic coupling between two metals, leading to a decrease of the electronic density on the metal. This evidence also indicates that the BiBzIm bridging ligand in the dinuclear complex has electron-donor ability.[46] The results are associated with the observation that the mononuclear compound **P3** is more efficiently quenched by TEOA than the dinuclear complex; however, the first oxidation potential of the dinuclear complex **P2** ($E_{1/2}$ = 1.03 V vs NHE) is higher than that of the mononuclear complex **P4** ($E_{1/2}$ = 0.81 V vs NHE). These results indicate that the BiBzIm bridging ligand in the dinuclear complex **P2** may be an electron acceptor. The observed oxidation potential of **P3** ($E_{1/2}$ = 0.73 V vs NHE) appeared close to that of **P5** ($E_{1/2}$ = 0.74 V vs NHE), which suggests that the contributions from the surrounding ligand with different electron donor/acceptor abilities of **P3** and **P5** to the HOMO energy levels are similar. These results are supported by the DFT calculations below, which indeed show similar HOMO energies for the two complexes. In contrast to the oxidation process, the reduction involving the addition of an electron to the lowest unoccupied molecular orbital (LUMO) was thought to occur at the surrounding electronegative ligands with little contribution from the iridium metal center. Upon reduction, all of the terdentate complexes showed the first wave with potentials in the range of −0.84 V to −1.07 V vs NHE, which were significantly positively shifted compared to those of the bidentate cyclometalated iridium complexes (−1.45 V to −1.56 V).

The above interpretations are further supported through DFT calculations. The electronic distribution between the HOMO and LUMO for each complex indicates an obvious intramolecular charge separation, as illustrated in Table 3. The

Table 3. HOMO and LUMO Distributions of Iridium Complexes P1−P5

Complex	HOMO	LUMO
P1	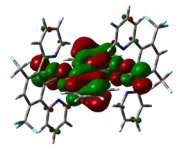	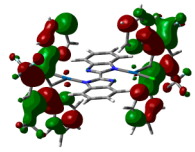
P2	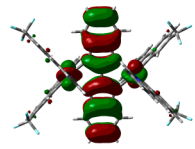	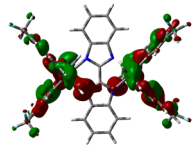
P3	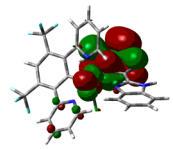	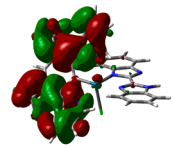
P4	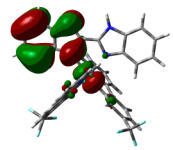	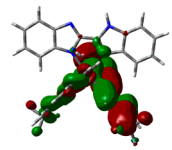
P5	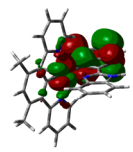	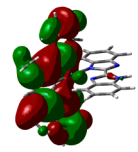

HOMO differs depending on the strength of the bonding properties of the ligand backbones. For the dinuclear complexes **P1** and **P2**, the HOMO is formed mainly from a combination of Ir 5d orbitals and the entire conjugated system of the BiBzIm bridging ligand, while the HOMO for the mononuclear complexes **P3**−**P5** originates from a combination of Ir 5d orbitals and half (cyclometalated fragments) of the BiBzIm ligand. Among the chloro complexes, there is significant

dx.doi.org/10.1021/cs500296s | ACS Catal. 2014, 4, 1953−1963

electron density on the monodentate halide ligand in the HOMO, which is expressed experimentally by the close oxidation potential between **P3** and **P5**. In contrast, the LUMO for N^C^N-containing complexes and C^N-containing complexes are mainly centered on the one N^C^N and two C^N ligands with little involvement of the Ir orbitals, respectively, which is consistent with the observed first reduction potentials staying in a narrow range in the related Ir complexes. On the basis of the results of DFT calculations, the excited state in these complexes can be approximately viewed as charge-transfer states mixed with MLCT/LLCT (ligand-to-ligand charge transfer) character.

Hydrogen Production Experiment. For applications in light-induced hydrogen production, the photoactive complex as a PS should have visible-light sensitivity and function as an efficient charge transfer sensitizer to the catalyst for water reduction. The electrochemical and photophysical results clearly indicated that all of the complexes have the potential to work as PSs in photochemical processes to reduce water into hydrogen. The dinuclear complexes are of particular interest because their absorption in the visible region is almost twice as intense as the mononuclear compounds. Such behavior is expected for compounds acting as PSs to make significant contributions to the system for solar energy conversion. To identify the dinuclear complexes as PSs, the photocatalytic reaction activities for hydrogen generation were assessed and compared to those of the mononuclear species, by adopting a three-component catalytic system in the presence of the water reduction catalyst (WRC) and TEOA as a sacrificial electron donor in a mixture of acetone and water. Quantitative determination of the generation of H_2 was conducted by GC analysis of the gas phase of the reaction system using a molecular sieve column with Ar as the carrier gas (for details, see the Experimental Section). The reaction turnover numbers [TONs = n(H)/n(PS)] were calculated according to one-electron transfer processes. The experimental results with value variables within less than 10% have repeatedly proven to be reproducible. No hydrogen was detected in the control experiments when PS, TEOA, or WRC was excluded from the system, demonstrating that all of the components are indispensable for the production of hydrogen in this system. Moreover, when the reaction was performed in the dark, no hydrogen was detected by GC analysis.

Initially, production of hydrogen occurred using $[Co(bpy)_3]Cl_2$ as a WRC upon irradiating deaerated solutions under visible light (Xe lamp with a cutoff filter, 300 W, λ > 420 nm). In a typical photocatalytic experiment, the three-component system was used in a 100 mL solution of water/acetone (1:4) containing PS (10 μM), $[Co(bpy)_3]Cl_2$ (0.33 mM), and TEOA (0.19 M) at a pH value lower than the pK_a of TEOA, pH = 8.0. The conditions were identical to those used for hydrogen photogeneration in our previous reports,[29,30] which have been optimized for the catalytic action of related PS compositions. The acetone/water mixed solvent was used to solubilize all of the components. The adjustment of pH value of the solution is accomplished by addition of hydrochloric acid. According to the previous related studies, the effect of the pH is complex and control of pH at the optimum level is required. The systems employing a cobalt catalyst, such as $[Co(bpy)_3]Cl_2$, have shown a pH-dependent activity for hydrogen evolution and perform as a more active WRC at approximately pH 8. At higher pH values, there is lower proton concentration and hydrogen production becomes more thermodynamically unfavorable. Moreover, this condition may inhibit hydrogen production because the cobalt hydride intermediate species, which are proposed to be the active species involving the observed photocatalysis, will be too stable to release hydrogen if the pH is too high.[51,52] On the contrary, lowering the pH value reduces the electron-donating ability of the protonated TEOA, offering an electron to the PS and thus reducing the reaction activity.

For all of the reported complexes, we measured their catalytic effectiveness in the reduction of water to hydrogen with a typical end-point reached after an irradiation time of 72 h for the dinuclear complexes **P1** and **P2** and 32 h for the mononuclear complexes **P3**–**P5**. These data are collected in Table 4. The photocatalytic capacity of the dinuclear complexes were superior to those of the mononuclear complexes under the given reaction conditions. When subjected to photolysis for a longer period of time, after 32 h irradiation, the dinuclear complexes **P1** and **P2** continued producing H_2, whereas the activity of the mononuclear complexes **P3** and **P4** slowed down substantially. After the hydrogen production experiment with **P3** had proceeded for 48 h, the system achieved a total hydrogen production of 27 μmol. For **P5**, no more hydrogen was produced upon extending the irradiation time. These results indicate that there is a correlation between the photophysical properties and catalytic activity. All fluorescing complexes are active for photocatalytic hydrogen production, while the low activity of **P5** was consistent with both the fluorescence intensity and the lifetime of the excited state. The catalytic activity and stability of the systems were improved when using the dinuclear complexes as PSs, which benefited from the photophysical properties and the relative symmetry of the molecular structures of these complexes. However, the TON was far less than for other previously reported mononuclear iridium-based photocatalytic systems,[53] in which synthetic modification and screening has been well established for improvement in catalytic activity and efficiency. Additionally, the TON depends strongly on the experimental conditions, such as the reaction scale, the experimental setup, the incident light power density, and so on. It should be taken into account that the reaction scale used in our experiments is different from most of the previous related reports. Our results are comparable to those of the related neutral homoleptic and heteroleptic cyclometalated Ir(III) complexes, which were measured in the same setup and identical conditions (10 μM PS, 100 mL solutions).[23,29,30] As described before, the k_q for the TEOA (**P1** and **P3**) is lower than that for the Co catalyst;

Table 4. Photocatalytic H_2-Producing Activity of Different Photosensitizers[a]

run	PS	H_2 (μmol)	TON
1[b]	**P1**	73	146
2[b]	**P2**	67	134
3[c]	**P3**	23	46
4[c]	**P4**	34	68
5[c]	**P5**	6	12
6[d]	$[Ir(tfm\text{-}ppy)_2(dtb\text{-}bpy)]^+$	74	148

[a]Photocatalytic conditions: 10 μM PS, 0.33 mM $[Co(bpy)_3]Cl_2$, and 0.19 M TEOA in acetone/water (4:1 v/v, 100 mL, pH 8.0) upon irradiation (Xe lamp; 300 W, λ > 420 nm). [b]Irradiation for 72 h. [c]Irradiation for 32 h. [d]Data taken from ref 23, where tfm-ppy =4-trifluoromethyl-2-phenylpyridine and dtb-bpy =4,4′-di-*tert*-butyl-2,2′-dipyridyl.

dx.doi.org/10.1021/cs500296s | ACS Catal. 2014, 4, 1953−1963

however, in the electron transfer step, reductive quenching still prevails over oxidative quenching because of the much higher concentration of TEOA (0.19 M) in the photoreactions compared with that of the catalyst (0.33 mM). For **P2** and **P4**, an oxidative quenching pathway in the photochemically driven step leads to H_2 evolution.

To improve the TON, a series of WRCs were evaluated under identical experimental conditions to those of the cobalt catalyst as described above. Among the iridium complexes tested, **P1** yielded the highest TONs and was used in subsequent studies compared to the corresponding mononuclear complex **P3**. The results are reported in Table 5. When the catalysis was carried out using the colloidal platinum catalyst generated in situ from K_2PtCl_4 under irradiation, both systems of **P1** and **P3** are active for hydrogen production. In the first hour, the system generated 23 μmol H_2 while using **P1**, after which the activity decreased significantly. After 5 h of irradiation, hydrogen production ceased, yielding 35 μmol H_2 in total. A dark solid particle was observed in the solution after the photocatalytic experiment, which may be aggregation of the colloidal platinum catalyst according to related reports. The results indicated that the systems were effective for hydrogen production through a reductive quenching pathway, which is compatible with the observed substantial quenching behavior. The chlorido-containing complexes, **P1** and **P3**, are seemingly neutral through the incorporation of negatively charged chlorido groups into the coordination sphere, confirmed by the ESI-MS data. However, the inclusion of a labile chloride ligand on the iridium center may modulate the cationic charge on the complexes in a controlled fashion, resulting in complexes with certain behavior as the cationic iridium complexes under the special conditions.[54] Subsequently, we chose $[Rh(dtb\text{-}bpy)_3](PF_6)_3$ as the WRC to study its activity toward hydrogen production. With **P1**, a total of 214 μmol H_2 was obtained with a TON of 428 after 32 h of irradiation. Though the long-term stability of the photocatalytic process was reduced, the system yielded more hydrogen when using $[Rh(dtb\text{-}bpy)_3](PF_6)_3$ instead of $[Co(bpy)_3]Cl_2$ as a WRC, which has previously been observed in the molecular system of hydrogen production.[30] Additionally, the use of $CoCl_2$ as a WRC was also attempted. For complex **P3**, in particular, it is expected that the complex spontaneously assembles with a Co(II) ion, making use of the free binding sites to form a supramolecular Ir−Co complex, as reported in the literature.[9] Unfortunately, this attempt failed as no appreciable amount of H_2 was obtained after 8 h of irradiation under the present conditions. The reason may be that the N−H proton on the BiBzImH ligand restrains the interactions between the Co metal center and the BiBzImH ligands. From the two series of experiments altering the WRC, $[Rh(dtb\text{-}bpy)_3](PF_6)_3$ was found to be the more active reduction catalyst than the others (K_2PtCl_4, $Co(bpy)_3Cl_2$, or $CoCl_2$) with these iridium complexes.

Table 5. Photocatalytic H_2-Producing Activity of P1 or P3 Using Different Catalysts[a]

run	PS	catalyst[b]	t (h)	H_2 (μmol)	TON
1	**P1**	[Co]	72	73	146
2	**P1**	K_2PtCl_4	5	35	70
3	**P1**	$CoCl_2$	8	0	0
4	**P1**	[Rh]	32	214	428
5	**P3**	[Co]	32	23	46
6	**P3**	K_2PtCl_4	5	9	18
7	**P3**	$CoCl_2$	8	0	0
8	**P3**	[Rh]	32	165	330

[a]Photocatalytic conditions: 10 μM PS, 0.33 mM catalyst and 0.19 M TEOA in acetone/water (4:1 v/v, 100 mL, pH 8.0) upon irradiation (Xe lamp, 300 W, λ > 420 nm). [b][Co] = $Co(bpy)_3Cl_2$. [Rh] = $Rh(dtb\text{-}bpy)_3(PF_6)_3$.

In light-induced catalytic experiments, the solvent plays a profound role in the activity and stability of the catalytic system. The ligating solvent influences the catalytic reaction by its ability to participate in the binding of the redox intermediates. This medium can also affect the photophysical properties of the excited state of PSs, such as energy, fluorescence quantum yield, lifetime and the rate of intermolecular electron transfer between PS and WRC. This effect is considered to be closely associated with the efficiency of hydrogen generation. A series of photocatalytic experiments based on the Ir−Rh-TEOA system by changing the ratio of acetone/water was carried out to study the effect of solvents with component concentrations of 10 μM **P1** or **P3**, 0.33 mM $[Rh(dtb\text{-}bpy)_3](PF_6)_3$, and 0.19 M TEOA at pH 8.0. For **P1**, a drastic solvent dependence for catalysis was observed, as shown in Figure 3A. When using the cosolvent acetone/water (9:1), the system with **P1** had the best performance with a total of 298 μmol H_2 (TON = 596) formed after 32 h irradiation. If using a higher water content in the acetone solution, the activity declined significantly. This result may be related to the intermolecular electron transfer rate,

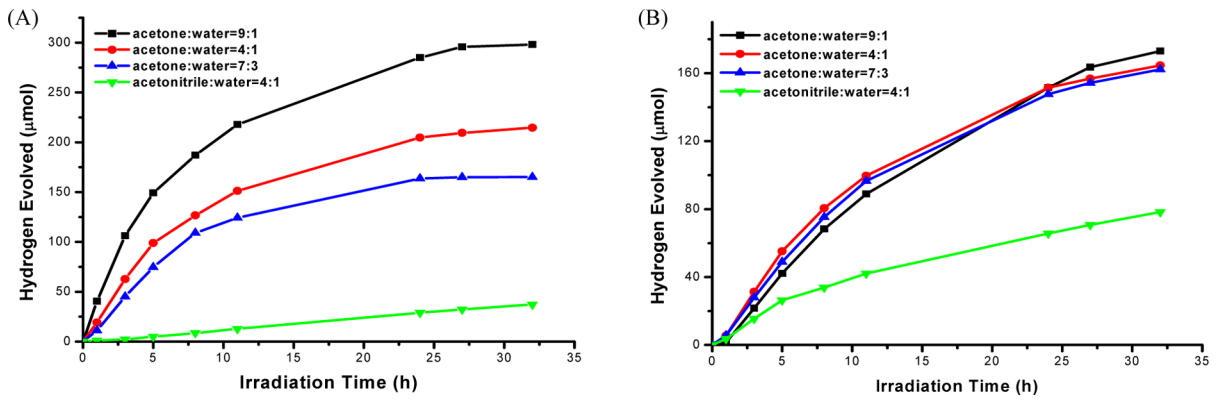

Figure 3. Photoinduced hydrogen production with different solvents at pH 8.0. Conditions: 0.33 mM $[Rh(dtb\text{-}bpy)_3](PF_6)_3$, 0.19 M TEOA, 10 μM **P1** (A) or **P3** (B), 100 mL solution (Xe lamp, 300 W, λ > 420 nm).

dx.doi.org/10.1021/cs500296s | ACS Catal. 2014, 4, 1953−1963

which is sensitive to changes in the dielectric constant of the solution. When using another polar solvent, acetonitrile, to replace acetone, the activity diminished, with the system yielding only 37 μmol H_2 after 32 h irradiation for **P1** (acetonitrile/water 4:1 v/v), which is a result of PS decomposition promoted by the ligating ability of the solvent.[20] When the photocatalytic reaction ceased, UV−vis spectra was conducted on a sample of the reaction mixture in acetone/water (9:1, v:v). The disappearance of the characteristic absorbance attributed to **P1** was observed compared with that prior to photolysis, suggesting the decomposition of **P1** occurs as hydrogen evolution. The evidence in regard to the instability of PS will be further discussed in the sections below. This finding was confirmed by the formation of a black solid after the photolysis.[25] However, when we performed the experiments with the corresponding mononuclear compound **P3**, the variation of the amount of water in the acetone solution did not have an obvious impact on the photocatalytic activity under the given conditions, as shown in Figure 3B. Similarly, the system did not retain photocatalytic activity in the mixed solvent solution of water/acetonitrile.

In a separate experiment, the stability of **P1** during photolysis was tested. At the end of a given hydrogen-producing cycle, the hydrogen was pumped out. As shown in Figure 4, the addition

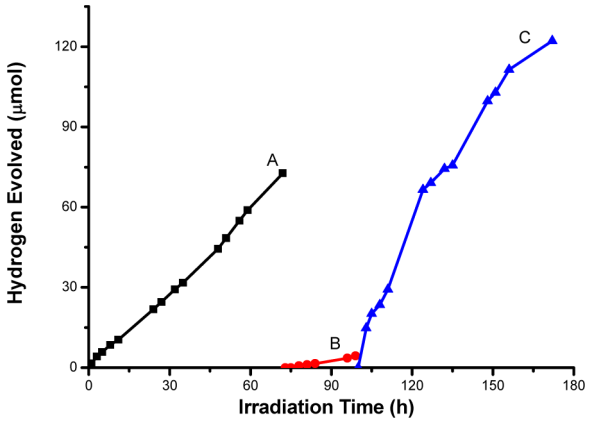

Figure 4. Hydrogen evolution vs time in an acetone/water (4:1 v/v) solvent containing 10 μM **P1**, 0.33 mM $Co(bpy)_3^{2+}$, and 0.19 M TEOA (pH = 8, λ > 420 nm). Trace A: the first 72 h irradiation. Trace B: further irradiation for 24 h after the injection of additional $Co(bpy)_3^{2+}$ (0.33 mM). Trace C: further irradiation for 72 h after the injection of additional **P1** (10 μM).

of an extra 1 equiv of catalyst failed to resume hydrogen production under illumination; only 4.4 μmol H_2 was obtained after irradiation of 24 h. When **P1** was readded (Figure 4, the blue curve), the activity was recovered with 244 TON H_2 after an additional 72 h of irradiation. The presence of the extra catalyst led to the increased performance of the system. The results implied that the chromophore decomposition, rather than catalyst deactivation, was the main reason for the cease of hydrogen evolution after illumination. The electrospray ionization-mass spectrometry (ESI-MS) analysis of the reaction mixture after the photocatalytic reaction clearly showed that the peak of complex **P1** (m/z = 1445.06) had disappeared (see the Supporting Information), indicating the occurrence of the decomposition of **P1** under the photocatalytic conditions, which was consistent with the above experimental results. The favored reductive quenching pathway in the present systems accounted for the photodegradation of the excited-state sensitizer and thus the limited stability of the reaction system.[8]

We also investigated the effect of the concentration of compounds **P1** and **P3** (1−20 μM) on the light-induced hydrogen production while the concentrations of TEOA (0.19 M) and catalyst kept constant at 0.19 M and 0.33 mM, respectively, in the mixed solvent solution of acetone/water (4:1 v/v, pH = 8.0). In the case of $Co(bpy)_3^{2+}$ as a catalyst (Table 6), when the photolysis experiment was conducted at

Table 6. Photocatalytic H_2-Producing Activity of Various Concentrations of P1 or P3 in the Presence of $Co(bpy)_3Cl_2$ as a Catalyst[a]

run	PS	concn (μM)	t (h)	H_2 (μmol)	TON
1	**P1**	1	72	87	1740
2	**P1**	5	72	66	264
3	**P1**	10	72	73	146
4	**P1**	20	72	286	286
5	**P3**	1	32	24	480
6	**P3**	5	32	22	88
7	**P3**	10	32	23	46
8	**P3**	20	32	36	36

[a]Photocatalytic conditions: a specified amount of PS, 0.33 mM $Co(bpy)_3Cl_2$ and 0.19 M TEOA in acetone/water (4:1 v/v, 100 mL, pH 8.0) upon irradiation (Xe lamp, 300 W, λ > 420 nm).

low concentrations of **P1** or **P3**, there was little influence on the overall evolution of hydrogen. The observation indicated that the activity of such systems may be intrinsically limited by the efficiency of the catalyst. Using 1 μM PS, a TON of 1740 based on **P1** can be achieved, whereas only 480 TON H_2 was obtained when **P3** was empolyed under the same conditions. Along with $[Rh(dtb\text{-}bpy)_3](PF_6)_3$ as a catalyst in the mixed solvent solution of acetone/water (9:1 v/v, pH = 8.0), as shown in Figure 5, increasing the PS concentration increased the total amount of hydrogen evolved for the system, suggesting that the activity was limited by the PS concentration. Using 1 μM PS, the system afforded a 3780 TON with respect to **P1** (1 μM), while the system based on **P3** was still much less efficient (TON = 1020) in the same conditions. When the concentration of PS was increased to 20 μM, a total of 598 and 495 μmol H_2 was produced for **P1** and **P3** in the catalytic system, respectively. The apparent quantum efficiency for the hydrogen production reaction was 1.02% and 0.45% at 420 nm over an irradiation time of 24 h for **P1** and **P3**, respectively (10 μM PS). Although it is known that molar absorptivity of the light-harvesting complex is essential for good performance of the solar-to-fuel conversion systems, there was little apparent correlation between photocatalytic behaviors and the photophysical properties of the sensitizers.[17,19] On the basis of the photophysical and electrochemical studies of **P1** and **P3**, molar absorptivity of the complex appears to be beneficial for the efficiency of the catalytic system presented here.

CONCLUSIONS

In this work, the synthesis of a new type of dinuclear iridium(III) complexes, the bridging ligands of which consist of two bidentate N−N chelates, were described. These charge-neutral complexes were thoroughly characterized, with the results indicating that they exhibit more intense absorption in visible light compared to their mononuclear analogues and have sufficient reduction potential to transfer an electron onto the

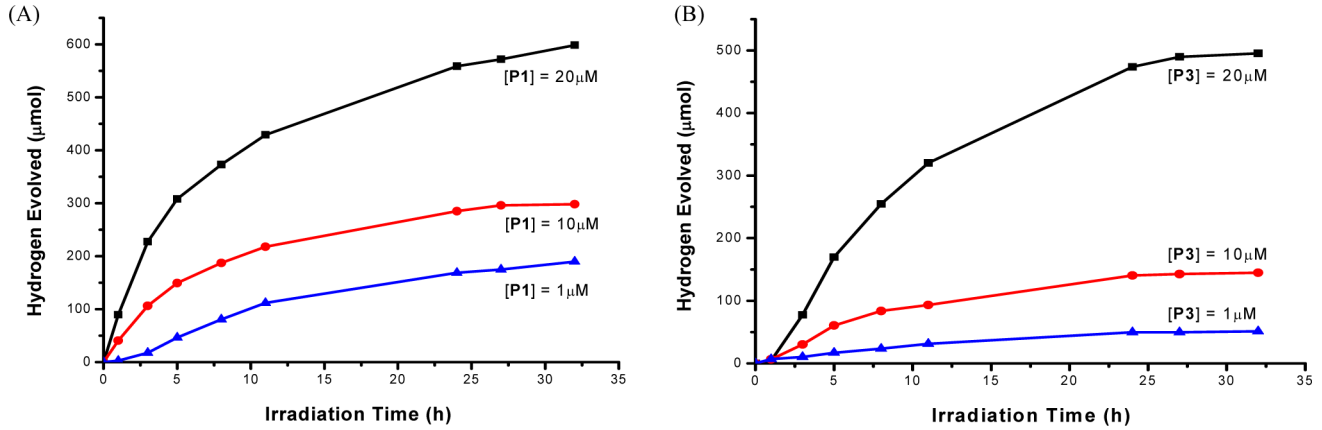

Figure 5. Photoinduced hydrogen production of various concentrations of **P1** (A) or **P3** (B) in acetone/water (9:1 v/v, 100 mL, pH 8.0). Conditions: 0.33 mM $[Rh(dtb\text{-}bpy)_3](PF_6)_3$ and 0.19 M TEOA (Xe lamp, 300 W, $\lambda > 420$ nm).

water reduction catalyst. The increase of absorption in the visible region of these chromophores appears most suitable for the application for light-induced photochemical reactions. The properties of the chlorido-containing complexes in solutions were different from others due to the presence of the labile chloride ligand. All of the complexes, including dinuclear and mononuclear compounds, were tested as photosensitizers for hydrogen generation with the help of a series of water reduction catalysts in photocatalytic experiments under pH = 8 conditions. The catalytic results indicated that enhancement of the photocatalytic reduction of water into hydrogen in the visible region was achieved by the dinuclear iridium complexes. However, the catalytic performance based on these new systems is far lower, in contrast to the previous reports. The development of new dinuclear coordination compounds can be anticipated to produce further superior results if additional structural modification and screening are performed. The results of this work, in connection with the dinuclear light-harvesting complexes, provide new information concerning the photophysical and structural requirements needed to build supramolecular metal complexes that can be used as PSs for artificial photosynthetic systems.

EXPERIMENTAL SECTION

General Measurements. The absorbance measurement was performed using a Varian Cary 50 UV−vis spectrophotometer for solutions. Emission spectra and luminescence quenching experiments were performed on a Varian Cary Eclipse fluorescence spectrophotometer. The fluorescence lifetime and the absolute quantum yield were acquired with a Horiba Jobin-Yvon FluoroMax-4 TCSPC spectrometer. ^{1}H NMR spectra were recorded on a Bruker AMX-500 MHz instrument. Mass spectra were obtained on a Thermo LCQ Fleet ESI-mass spectrometer. The electrochemical properties of these complexes in anhydrous acetonitrile were investigated in a traditional three-electrode cell consisting of a glassy carbon disk (3 mm diameter disk) working electrode, an auxiliary platinum wire, and an Ag/AgCl (saturated KCl) reference electrode using a PARSTAT-2273 advanced electrochemical system. Diffraction intensity data for single crystals of complexes **P2** and **P4**, which were obtained by slow diffusion of hexane into a CH_2Cl_2 solution, were collected at room temperature on a Bruker Smart CCD diffractometer equipped with graphite monochromated Mo Kα radiation (λ = 0.71073 Å). The structures were solved by the direct method and refined by the full-matrix least-squares method on F_2 with anisotropic thermal parameters for all non-hydrogen atoms. Poor crystal structure refinements for **P2** cannot be improved due to relatively low-quality crystals. Density functional calculations (B3LYP/LANL2DZ) were performed by using Guassian 09. The numerical calculations in this paper were performed on the IBM Blade cluster system at the High Performance Computing Center (HPCC) of Nanjing University.

H_2 Evolution Experiments. All H_2 production experiments were evaluated in a Pyrex vessel with a side visible light irradiation using a 300 W xenon lamp equipped with a cutoff filter (radiation wavelength >420 nm), as described previously.[21,22] The reactor was charged with 10 μM PS, 0.33 mM catalyst, and 0.19 M TEOA (2.5 mL) in an aqueous solution (100 mL) with gentle magnetic stirring. The pH value was adjusted to approximately 8.0 by the addition of concentrated hydrochloric acid. Prior to light irradiation, the system was evacuated successively before being backfilled with argon. The evolved gas was periodically detected on a gas chromatograph equipped with a thermally conductive detector (Shimadzu GC-8A, argon as a carrier gas and MS-5A column). The apparent quantum efficiency (QE) for the photocatalytic reaction was measured under irradiation of monochromatized light at 420 nm.[21]

Synthetic Procedure for Iridium Complexes. The corresponding dichloro-bridged dimers were synthesized using a known method.[55] $BiBzImH_2$ was also synthesized as reported in the literature.[56] Commercial chemicals were used as supplied.

$[Ir(tfdpyb)Cl]_2(BiBzIm)$ (P1) and Ir(tfdpyb)(BiBzImH)Cl (P3). A mixture of $[Ir(tfdpyb)Cl)]_2$ (400 mg, 0.38 mmol), 2,2′-bibenzimidazole (192 mg, 0.82 mmol), and Na_2CO_3 (396 mg, 3.8 mmol) in 30 mL of CH_3OH/CH_2Cl_2 (1:1) was refluxed under an atmosphere of nitrogen for 24 h. After cooling to room temperature, the solvent was removed under reduced pressure, and the crude product was purified by chromatography on silica (hexane/EtOAc (1:1) to EtOAc) to afford the products **P1** (122 mg) and **P3** (212 mg).

P1: ^{1}H NMR (DMSO, 500 MHz): δ 8.46 (4H, d, J = 8.3), δ 8.27 (2H, s), δ 8.12 (4H, t, J = 7.7), δ 7.94 (4H, d, J = 5.3), δ 7.87 (2H, d, J = 8.0), δ 7.39 (4H, t, J = 6.5), δ 7.04 (2H, t, J = 7.5), δ 6.86 (2H, t, J = 7.8), δ 5.37 (2H, d, J = 8.4). ESI-MS (CH_3OH): m/z 1445.25 $[M + Na]^+$; calcd for $C_{50}H_{26}N_8F_{12}Cl_2NaIr_2$, 1445.06.

dx.doi.org/10.1021/cs500296s | ACS Catal. 2014, 4, 1953−1963

P3: ^{1}H NMR (DMSO, 500 MHz): δ 8.65 (1H, d, J = 8.2), δ 8.38 (2H, d, J = 8.4), δ 8.22 (1H, s), δ 8.15 (2H, d, J = 5.3), δ 8.05 (2H, t, J = 7.9), δ 7.84 (1H, d, J = 8.2), δ 7.54 (1H, t, J = 7.7), δ 7.46 (1H, t, J = 7.6), δ 7.41 (2H, t, J = 6.6), δ 7.35 (1H, d, J = 8.1), δ 6.80 (1H, t, J = 7.5), δ 6.55 (1H, t, J = 7.7), δ 5.13 (1H, d, J = 8.4). ESI-MS (CH_3OH): m/z 829.42 $[M + H]^+$; calcd for $C_{32}H_{19}N_6ClF_6Ir$, 829.08. HRMS (CH_3OH): m/z 829.0921 $[M + H]^+$; calcd for $C_{32}H_{19}N_6ClF_6Ir$, 829.0894.

[Ir(tfmppy)$_2$]$_2$BiBzIm (P2) and Ir(tfmppy)$_2$(BiBzIm)(P4). Similar to the above procedure, the reaction starting from $[Ir(tfmppy)_2Cl]_2$ (300 mg, 0.25 mmol), 2,2′-bibenzimidazole (129 mg, 0.55 mmol), and Na_2CO_3 (198 mg, 1.8 mmol) in 30 mL CH_3OH/CH_2Cl_2 (1:1) gave the products **P2** (82 mg) and **P5** (182 mg).

P2: ^{1}H NMR (DMSO, 500 MHz): δ 8.39 (4H, d, J = 8.2), δ 8.11 (4H, d, J = 8.2), δ 7.97 (4H, t, J = 7.8), δ 7.62 (4H, d, J = 5.7), δ 7.38 (4H, t, J = 8.0), δ 7.15 (4H, t, J = 6.6), δ 6.66 (4H, m, J = 3.1), δ 6.61 (4H, s), δ 5.87 (4H, m, J = 3.1). ESI-MS (CH_3OH): m/z 1507.08 $[M + H]^+$; calcd for $C_{62}H_{37}N_8F_{12}Ir_2$, 1507.21.

P4: ^{1}H NMR (DMSO, 500 MHz): δ 8.33 (2H, d, J = 8.2), δ 8.13 (2H, d, J = 8.2), δ 7.90 (2H, t, J = 7.4), δ 7.76 (2H, d, J = 5.5), δ 7.56 (2H, d, J = 8.1), δ 7.38 (2H, d, J = 7.9), δ 7.25 (2H, t, J = 6.6), δ 7.08 (2H, t, J = 7.6), δ 6.78 (2H, t, J = 7.6), δ 6.61 (2H, s), δ 5.89 (2H, d, J = 8.3). ESI-MS (CH_3OH): m/z 871.42 $[M + H]^+$, calcd for $C_{38}H_{24}N_6F_6Ir$: m/z 871.15. HRMS (CH_3OH): m/z 871.1635 $[M + H]^+$; calcd for $C_{38}H_{24}N_6F_6Ir$, 871.1597.

Ir(dpyx)(BiBzImH)Cl (P5). A mixture of $[Ir(dpyx)Cl]_2$ (200 mg, 0.19 mmol), 2,2′-bibenzimidazole (98 mg, 0.42 mmol), and AgOTf (261 mg, 0.88 mmol) in toluene (30 mL) was refluxed under a nitrogen atmosphere for 24 h. After the precipitated AgCl was filtered and washing with CH_2Cl_2, the solutions were combined, and the solvent was removed under reduced pressure. The residue was purified by chromatography on silica (CH_3OH/CH_2Cl_2 (1:10)) to give a yellow solid. The solid can be purified by recrystallization from the solution (10:1 CH_2Cl_2/CH_3OH), giving a yellow solid (112 mg).

P5: ^{1}H NMR (DMSO, 500 MHz): δ 8.68 (1H, d, J = 8.0), δ 8.14 (2H, d, J = 8.2), δ 7.88 (2H, d, J = 4.9), δ 7.80 (1H, d, J = 8.0), δ 7.75 (2H, t, J = 3.8), δ 7.50 (1H, t, J = 7.5), δ 7.43 (1H, t, J = 7.4), δ 7.32 (1H, d, J = 7.9), δ 7.15 (1H, s), δ 7.10 (2H, t, J = 6.3), δ 6.78 (1H, t, J = 7.3), δ 6.50 (1H, t, J = 7.5), δ 5.41(1H, d, J = 8.2), δ 2.86 (6H, s). ESI-MS (CH_3OH): m/z 721.42 $[M + H]^+$; calcd for $C_{32}H_{25}N_6ClIr$, 721.14. HRMS (CH_3OH): m/z 721.2597 $[M + H]^+$; calcd for $C_{32}H_{25}N_6ClIr$, 721.1459.

■ ASSOCIATED CONTENT

Supporting Information

Full experimental details and additional characterization data including emission decay kinetics, CVs, and Stern−Volmer plot for emission quenching for all complexes in this work. This material is available free of charge via the Internet at http://pubs.acs.org.

■ AUTHOR INFORMATION

Corresponding Author

*E-mail: yuzt@nju.edu.cn.

Notes

The authors declare no competing financial interest.

■ ACKNOWLEDGMENTS

This work was financially supported by the National Basic Research Program of China (Grant No. 2013CB632400), the National Science Foundation of China (Grant No. 20901038), and the Fundamental Research Funds for the Central Universities. We are also grateful to the Scientific Research Foundation for the Returned Overseas Chinese Scholars, State Education Ministry.

■ REFERENCES

(1) Frischmann, P. D.; Mahata, K.; Würthner, F. *Chem. Soc. Rev.* **2013**, *42*, 1847−1870.
(2) Sun, L.; Hammarström, L.; Åkermark, B.; Styring, S. *Chem. Soc. Rev.* **2001**, *30*, 36−49.
(3) Artero, V.; Chavarot-Kerlidou, M.; Fontecave, M. *Angew. Chem., Int. Ed.* **2011**, *50*, 7238−7266.
(4) Wang, M.; Na, Y.; Gorlov, M.; Sun, L. *Dalton Trans.* **2009**, 6458−6467.
(5) Krassen, H.; Ott, S.; Heberle, J. *Phys. Chem. Chem. Phys.* **2011**, *13*, 47−57.
(6) Fukuzumi, S.; Yamada, Y.; Suenobu, T.; Ohkubo, K.; Kotani, H. *Energy Environ. Sci.* **2011**, *4*, 2754−2766.
(7) Luo, S. P.; Mejía, E.; Friedrich, A.; Pazidis, A.; Junge, H.; Surkus, A. E.; Jackstell, R.; Denurra, S.; Gladiali, S.; Lochbrunner, S.; Beller, M. *Angew. Chem., Int. Ed.* **2013**, *52*, 419−423.
(8) Han, Z.; McNamara, W. R.; Eum, M. S.; Holland, P. L.; Eisenberg, R. *Angew. Chem., Int. Ed.* **2012**, *51*, 1667−1670.
(9) Jasimuddin, S.; Yamada, T.; Fukuju, K.; Otsuki, J.; Sakai, K. *Chem. Commun.* **2010**, *46*, 8466−8468.
(10) Zhang, P.; Jacques, P. A.; Chavarot-Kerlidou, M.; Wang, M.; Sun, L.; Fontecave, M.; Artero, V. *Inorg. Chem.* **2012**, *51*, 2115−2120.
(11) Zhang, P.; Wang, M.; Na, Y.; Li, X.; Jiang, Y.; Sun, L. *Dalton Trans.* **2010**, *39*, 1204−1206.
(12) Li, X.; Wang, M.; Zheng, D.; Han, K.; Dong, J.; Sun, L. *Energy Environ. Sci.* **2012**, *5*, 8220−8224.
(13) Wang, M.; Chen, L.; Sun, L. *Energy Environ. Sci.* **2012**, *5*, 6763−6778.
(14) Wenger, O. S. *Coord. Chem. Rev.* **2009**, *253*, 1439−1457.
(15) Gärtner, F.; Boddien, A.; Barsch, E.; Fumino, K.; Losse, S.; Junge, H.; Hollmann, D.; Brückner, A.; Ludwig, R.; Beller, M. *Chem.—Eur. J.* **2011**, *17*, 6425−6436.
(16) Gärtner, F.; Cozzula, D.; Losse, S.; Boddien, A.; Anilkumar, G.; Junge, H.; Schulz, T.; Marquet, N.; Spannenberg, A.; Gladiali, S.; Beller, M. *Chem.—Eur. J.* **2011**, *17*, 6998−7006.
(17) Gärtner, F.; Denurra, S.; Losse, S.; Neubauer, A.; Boddien, A.; Gopinathan, A.; Spannenberg, A.; Junge, H.; Lochbrunner, S.; Blug, M.; Hoch, S.; Busse, J.; Gladiali, S.; Beller, M. *Chem.—Eur. J.* **2012**, *18*, 3220−3225.
(18) Goldsmith, J. I.; Hudson, W. R.; Lowry, M. S.; Anderson, T. H.; Bernhard, S. *J. Am. Chem. Soc.* **2005**, *127*, 7502−7510.
(19) Brooks, A. C.; Basore, K.; Bernhard, S. *Inorg. Chem.* **2013**, *52*, 5794−5800.
(20) Tinker, L. L.; Bernhard, S. *Inorg. Chem.* **2009**, *48*, 10507−10511.
(21) Yuan, Y. J.; Yu, Z. T.; Chen, X. Y.; Zhang, J. Y.; Zou, Z. G. *Chem.—Eur. J.* **2011**, *17*, 12891−12895.
(22) Yuan, Y. J.; Zhang, J. Y.; Yu, Z. T.; Feng, J. Y.; Luo, W. J.; Ye, J. H.; Zou, Z. G. *Inorg. Chem.* **2012**, *51*, 4123−4133.
(23) Yu, Z. T.; Yuan, Y. J.; Cai, J. G.; Zou, Z. G. *Chem.—Eur. J.* **2013**, *19*, 1303−1310.
(24) You, Y.; Nam, W. *Chem. Soc. Rev.* **2012**, *41*, 7061−7084.
(25) Tinker, L. J.; McDaniel, N. D.; Curtin, P. N.; Smith, C. K.; Ireland, M. J.; Bernhard, S. *Chem.—Eur. J.* **2007**, *13*, 8726−8732.
(26) Metz, S.; Bernhard, S. *Chem. Commun.* **2010**, *46*, 7551−7553.
(27) DiSalle, B. F.; Bernhard, S. *J. Am. Chem. Soc.* **2011**, *133*, 11819−11821.
(28) Hansen, S.; Pohl, M. M.; Klahn, M.; Spannenberg, A.; Beweries, T. *ChemSusChem* **2013**, *6*, 92−101.

(29) Yuan, Y. J.; Yu, Z. T.; Gao, H. L.; Zou, Z. G.; Zheng, C.; Huang, W. *Chem.—Eur. J.* **2013**, *19*, 6340−6349.
(30) Yuan, Y. J.; Yu, Z. T.; Cai, J. G.; Zheng, C.; Huang, W.; Zou, Z. G. *ChemSusChem* **2013**, *6*, 1357−1365.
(31) Donato, L.; McCusker, C. E.; Castellano, F. N.; Zysman-Colman, E. *Inorg. Chem.* **2013**, *52*, 8495−8504.
(32) Auffrant, A.; Barbieri, A.; Barigelletti, F.; Lacour, J.; Mobian, P.; Collin, J.-P.; Sauvage, J.-P.; Ventura, B. *Inorg. Chem.* **2007**, *46*, 6911−6919.
(33) Auffrant, A.; Barbieri, A.; Barigelletti, F.; Collin, J.-P.; Flamigni, L.; Sabatini, C.; Sauvage, J.-P. *Inorg. Chem.* **2006**, *45*, 10990−10997.
(34) Welter, S.; Lafolet, F.; Cecchetto, E.; Vergeer, F.; De Cola, L. *ChemPhysChem* **2005**, *6*, 2417−2427.
(35) Plummer, E. A.; Hofstraat, J. W.; De Cola, L. *Dalton Trans.* **2003**, 2080−2084.
(36) Indelli, M. T.; Bura, T.; Ziessel, R. *Inorg. Chem.* **2013**, *52*, 2918−2926.
(37) Andreiadis, E. S.; Imbert, D.; Pécaut, J.; Calborean, A.; Ciofini, I.; Adamo, C.; Demadrille, R.; Mazzanti, M. *Inorg. Chem.* **2011**, *50*, 8197−8206.
(38) Barcina, J. O.; Herrero-García, N.; Cucinotta, F.; De Cola, L.; Contreras-Carballada, P.; Williams, R. M.; Guerrero-Martínez, A. *Chem.—Eur. J.* **2010**, *16*, 6033−6040.
(39) McCusker, C. E.; Hablot, D.; Ziessel, R.; Castellano, F. N. *Inorg. Chem.* **2012**, *51*, 7957−7959.
(40) Costa, R. D.; Fernández, G.; Sánchez, L.; Martín, N.; Ortí, E.; Bolink, H. J. *Chem.—Eur. J.* **2010**, *16*, 9855−9863.
(41) Tsuboyama, A.; Takiguchi, T.; Okada, S.; Osawa, M.; Hoshino, M.; Ueno, K. *Dalton Trans.* **2004**, 1115−1116.
(42) Whittle, V. L.; Williams, J. A. G. *Inorg. Chem.* **2008**, *47*, 6596−6607.
(43) Hags, M.; Matsumura-Inoue, T.; Yamabe, S. *Inorg. Chem.* **1987**, *26*, 4148−4154.
(44) Rillema, D. P.; Sahai, R.; Matthews, P.; Edwards, A. K.; Shaver, R. J.; Morgan, L. *Inorg. Chem.* **1990**, *29*, 167−175.
(45) Haga, M.; Bond, A. M. *Inorg. Chem.* **1991**, *30*, 475−480.
(46) Yin, J.; Elsenbaumer, R. L. *Inorg. Chem.* **2007**, *46*, 6891−6901.
(47) Brulatti, P.; Gildea, R. J.; Howard, J. A. K.; Fattori, V.; Cocchi, M.; Williams, J. A. G. *Inorg. Chem.* **2012**, *51*, 3813−3826.
(48) Zhu, Y. C.; Zhou, L.; Li, H. Y.; Xu, Q. L.; Teng, M. Y.; Zheng, Y. X.; Zuo, J. L.; Zhang, H. J.; You, X. Z. *Adv. Mater.* **2011**, *23*, 4041−4046.
(49) Wilkinson, A. J.; Puschmann, H.; Howard, J. A. K.; Foster, C. E.; Williams, J. A. G. *Inorg. Chem.* **2006**, *45*, 8685−8699.
(50) Wilkinson, A. J.; Goeta, A. E.; Foster, C. E.; Williams, J. A. G. *Inorg. Chem.* **2004**, *43*, 6513−6515.
(51) Zhang, P.; Wang, M.; Dong, J.; Li, X.; Wang, F.; Wu, L.; Sun, L. *J. Phys. Chem. C* **2010**, *114*, 15868−15874.
(52) Marinescu, S. C.; Winkler, J. R.; Gray, H. B. *Proc. Natl. Acad. Sci. U.S.A.* **2012**, *109*, 15127−15131.
(53) Whang, D. R.; Sakai, K.; Park, S. Y. *Angew. Chem., Int. Ed.* **2013**, *52*, 11612−11615.
(54) Pandrala, M.; Li, F.; Feterl, M.; Mulyana, Y.; Warner, J. M.; Wallace, L.; Keene, F. R.; Collins, J. G. *Dalton Trans.* **2013**, *42*, 4686−4694.
(55) Nonoyama, M. *Bull. Chem. Soc. Jpn.* **1974**, *47*, 767−768.
(56) Huang, W. K.; Cheng, C. W.; Chang, S. M.; Lee, Y. P.; Diau, E. W. G. *Chem. Commun.* **2010**, *46*, 8992−8994.